# Intracellular Folding Pathway of the Cystine Knot-Containing Glycoprotein Hormone α-Subunit†

Ryan J. Darling,‡ Jason A. Wilken,§ Raymond W. Ruddon,‡,|| and Elliott Bedows*,‡,§,⊥

*Department of Pharmacology, Department of Biochemistry and Molecular Biology, and Department of Obstetrics and Gynecology, Eppley Institute for Research in Cancer and Allied Diseases, University of Nebraska Medical Center, Omaha, Nebraska 68198-6805*

*Received August 29, 2000; Revised Manuscript Received November 2, 2000*

ABSTRACT: Three of the five disulfide bonds in the glycoprotein hormone α-subunit (GPH-α) form a cystine knot motif that stabilizes a three-loop antiparallel structure. Previously, we described a mutant ($\alpha_k$) that contained only the three knot disulfide bonds and demonstrated that the cystine knot was necessary and sufficient for efficient GPH-α folding and secretion. In this study, we used $\alpha_k$ as a model to study the intracellular GPH-α folding pathway. Cystine knot formation proceeded through a 1-disulfide intermediate that contained the 28−82 disulfide bond. Formation of disulfide bond 10−60, then disulfide bond 32−84, followed the formation of 28−82. Whether the two non-cystine knot bonds 7−31 and 59−87 could form independent of the knot was also tested. Disulfide bond 7−31 formed rapidly, whereas 59−87 did not form when all cysteine residues of the cystine knot were converted to alanine, suggesting that 7−31 forms early in the folding pathway and that 59−87 forms during or after cystine knot formation. Finally, loop 2 of GPH-α has been shown to be very flexible, suggesting that loop 2 does not actively drive GPH-α folding. To test this, we replaced residues 36−55 in the flexible loop 2 with an artificially flexible glycine chain. Consistent with our hypothesis, folding and secretion were unaffected when loop 2 was replaced with the glycine chain. Based on these findings, we describe a model for the intracellular folding pathway of GPH-α and discuss how these findings may provide insight into the folding mechanisms of other cystine knot-containing proteins.

The common glycoprotein hormone α-subunit (GPH-α)[1] is a 92-amino acid subunit that combines with 4 distinct *β*-subunits. The four resulting hormones are human chorionic gonadotropin (hCG), luteinizing hormone, follicle-stimulating hormone, and thyroid-stimulating hormone. GPH-α contains five disulfide (S−S) bonds in its native conformation. The cysteine pairings, based on crystallographic data (*1*, *2*), are $Cys^{7}$−$Cys^{31}$, $Cys^{59}$−$Cys^{87}$, $Cys^{28}$−$Cys^{82}$, $Cys^{10}$−$Cys^{60}$, and $Cys^{32}$−$Cys^{84}$ (Figure 1). Two of these S−S bonds (28−82 and 32−84) create an 8-amino acid ring by bridging adjacent polypeptide strands. A third S−S bond (10−60) penetrates this ring. This structural motif is termed a cystine knot and is common to a number of proteins, including hCG-*β*, transforming growth factor-*β*, nerve growth factor, platelet-derived growth factor [for reviews, see refs (*3*, *4*)], and vascular endothelial growth factor (*5*). While the topologies of these molecules are strikingly similar, the biological functions are diverse, suggesting that the cystine knot is a molecular scaffold upon which numerous functional domains are built (*3*). The functional significance of the cystine knot is demonstrated by the loss-of-function that results following site-directed mutagenesis of cystine knot residues (*6*−*9*) and naturally occurring mutations (*10*−*12*) that disrupt the cystine knot motif. A similar cystine knot is also present in the family of macrocyclic peptides (cyclotides) isolated from plants. Recently, folding studies of acyclic permutants of kalata B1, a prototypic cyclotide, have demonstrated that folding is dependent upon an intact cystine knot (*13*). This is consistent with our previous reports where disruption of either the GPH-α cystine knot (*6*) or the hCG-*β* cystine knot (*7*, *14*) resulted in subunit misfolding. These observations demonstrate that the cystine knot motif is vital to the biological function of numerous proteins.

GPH-α also contains two non-cystine knot S−S bonds (7−31 and 59−87) that are located in the N- and C-terminal domains, respectively (Figure 1). Recently, we reported that removal of S−S bond 7−31, bond 59−87, or both (leaving only the cystine knot) did not disrupt GPH-α cystine knot formation, folding, or secretion (*6*). This was, to the best of

† This material is based upon work supported in part by NIH Grant CA32949 (to E.B.), by a National Science Foundation Graduate Fellowship (to R.J.D.), and by NCI Cancer Center Support Grant P 30 CA36727 to the Eppley Institute.

* To whom correspondence should be addressed at the Eppley Institute for Research in Cancer and Allied Diseases, University of Nebraska Medical Center, 986805 Nebraska Medical Center, Omaha, NE 68198-6805. Tel.: 402-559-6074; Fax: 402-559-4651; E-mail: ebedows@unmc.edu.

‡ Department of Pharmacology.

§ Department of Biochemistry and Molecular Biology.

|| Current address: Corporate Office of Science and Technology, Johnson & Johnson, 410 George St., New Brunswick, NJ 08901.

⊥ Department of Obstetrics and Gynecology.

[1] Abbreviations: GPH-α, glycoprotein hormone α-subunit; hCG, human chorionic gonadotropin; S−S, disulfide; DTT, dithiothreitol; PBS, phosphate-buffered saline; NEM, *N*-ethylmaleimide; PAGE, polyacrylamide gel electrophoresis; HPLC, high-performance liquid chromatography; WT, wild type.

10.1021/bi002046a CCC: $20.00 
Published on Web 12/15/2000

our knowledge, the first report of a protein constructed to contain a growth factor cystine knot without any additional S−S bonds. Here, we used this modified α-subunit (termed $\alpha_k$) as a model to determine the mechanism of cystine knot formation. Additionally, we investigated the importance of the cystine knot in the formation of the two non-cystine knot GPH-α S−S bonds, 7−31 and 59−87. Because the cystine knot is a common motif in more than 30 proteins, the results presented in this study may provide insight into folding mechanisms of cystine knot-containing proteins in general.

Another particularly interesting domain of GPH-α is loop 2, which consists of residues 33−58 (Figure 1). Loop 2 is flexible in the free GPH-α subunit, containing an undefined structure (*15*, *16*). This flexibility also has interesting implications for understanding the mechanism of GPH-α folding because it links the more structurally rigid N- and C-terminal domains. This type of conformational arrangement (i.e., two structural domains linked by a flexible region) implies that GPH-α folding may fit a diffusion−collision model of folding (*17*). In this model, two structural domains diffuse randomly until proper interactions are stabilized by interdomain contacts. Thus, formation of a flexible loop is a byproduct of the folding process. Replacement of flexible loops with artificially flexible poly-glycine linkers has been used to study the role of loops in the folding of proteins such as Rop (*18*, *19*) and chymotrypsin inhibitor-2 (*20*), as well as the SH3 domain of α-spectrin (*21*). In this report, we use a similar strategy to show that replacement of 20 residues to the flexible GPH-α loop 2 with 20 glycine residues has no detectable effect on the subunit folding or secretion, suggesting that loop 2 plays a passive role in folding.

In this study, we describe the intracellular folding pathway of GPH-α and the mechanism for GPH-α cystine knot formation. These novel findings now extend our understanding of cystine knot formation and should aid in understanding the folding of the growth factor superfamily of cystine knot-containing proteins.

## EXPERIMENTAL PROCEDURES

*Cell Culture.* 293T cells (*22*) were grown in Dulbecco's modified Eagle's medium (Life Technologies, Inc.) supplemented with 10% fetal bovine serum, and penicillin (100 units/mL)/streptomycin (100 μg/mL) (Life Technologies, Inc.).

*Site-Directed Mutagenesis and Expression of Recombinant GPH-α.* To remove a particular S−S bond, cysteine pairs were converted to alanine. Since all cysteine residues are paired in GPH-α, substitutions to alanine were generated in pairs so that free thiols were not generated, which could facilitate S−S bond rearrangements. Previously, mutation to either alanine or serine gave the same results when hCG-β folding was studied (*23*), suggesting the changes in folding were indeed due to disrupting S−S bond formation. Conversion of cysteine residues to alanine was performed using a megaprimer polymerase chain reaction methodology (*24*). A 410-base pair fragment was cloned into the pcDNA3 vector (Invitrogen) using *Hin*dIII and *Apa*I restriction sites. To create the α(GlyL2) construct, a sense primer containing a 5′ *Xba*I site (corresponding to codons 34−35) followed by 20 Gly codons and a 3′ complementary region (codons 56−67) was used with SP6 primer in a polymerase chain reaction. The product was ligated into pcDNA3-α using *Xba*I and *Apa*I sites. DNA sequencing confirmed the fidelity of the desired mutations. Plasmid DNA was purified using a Maxi Plasmid Kit (Qiagen) according to the manufacture's protocol and was used for transient transfection as described below. The construct containing only the six cysteine residues that form the cystine knot S−S bonds was termed $\alpha_k$ and contained C7A, C31A, C59A, and C87A mutations. Further removal of S−S bonds from $\alpha_k$ was designated as $\alpha_k$C*x*-*y*A, where *x* and *y* indicate the cysteine residue numbers that were converted to alanine. The variant containing only cysteines 7, 31, 59, and 87 (lacking all cysteine residues that form the knot) was termed α7−31/59−87.

*Transient Transfection.* 293T cells ($1.9 \times 10^6$) were plated into 60-mm plastic dishes and grown overnight at 37 °C to 70−80% confluency. Plasmid DNA was precipitated as described previously (*6*). For coexpression of hCG-β with GPH-α, pcDNA3-hCGβ (*6*) was included in the precipitation. The resulting precipitate was added dropwise to a 60-mm dish of 293T cells and agitated gently to mix. To ensure a uniform precipitate exposure, one large-scale precipitation was used and distributed equally among all dishes. The cells were incubated for 2 days at 37 °C and used for metabolic labeling.

*Metabolic Labeling with [$^{35}$S]Cysteine.* Transiently transfected 293T cells were pulse-labeled for the times indicated in the text with L-[$^{35}$S]cysteine (∼1100 Ci/mmol; NEN Life Science Products), at a final concentration of 100−150 μCi/mL in serum-free medium lacking cysteine (*7*). For experiments using dithiothreitol (DTT), DTT was added with the [$^{35}$S]cysteine at a final concentration of 2.0 mM. Pulse incubations were carried out as described previously (*6*, *25*), and the cells were incubated for the chase times indicated in the text. For secretion studies, the chase medium was saved. Cells were harvested by rinsing with cold phosphate-buffered saline (PBS) and immediately lysed in 2.5 mL of PBS containing detergents (1.0% Triton X-100, 0.5% sodium deoxycholate, and 0.1% SDS), protease inhibitors (20 mM EDTA and 2 mM phenylmethanesulfonyl fluoride), and 5 mM *N*-ethylmaleimide (NEM), pH 7.0, to trap free thiols in the GPH-α folding intermediates that contained unformed S−S bonds. Cell lysates were incubated for 10−20 min at room temperature in the dark followed by disruption through a 22-gauge needle (5 times) and centrifugation for 1 h at 100000*g*. For secretion studies, the chase medium was clarified by centrifugation for 10 min at 100000*g*.

*Immunoprecipitation of Cell Lysates and Culture Media.* Immunoreactive forms of GPH-α were immunoprecipitated with a polyclonal rabbit antibody that recognizes all known forms of GPH-α (*6*). Immunoprecipitations were carried out at 4 °C for 16−20 h with rotation in the dark. Immune complexes were precipitated with protein A−Sepharose (Sigma) and prepared for SDS−polyacrylamide gel electrophoresis (PAGE) or reversed-phase high-performance liquid chromatography (HPLC) as described below.

*Reversed-Phase HPLC Analysis.* Radiolabeled GPH-α forms that adsorbed to protein A−Sepharose beads were prepared as described previously (*25*). Briefly, protein A−Sepharose beads/antibody−antigen immunocomplexes were washed 3 times with PBS containing detergents (1% Triton X-100, 0.5% sodium deoxycholate, 0.1% SDS)

followed by 3 washes with PBS lacking detergents. Immunocomplexes were pelleted between washes by centrifugation for 1 min at 2000*g*. To dissociate the precipitated immunocomplexes, pellets were treated with 6 M guanidine hydrochloride, pH 3.0 (sequenal grade; Pierce), for 16−20 h while rotating at room temperature. Then 100 $\mu$g of myoglobin was added as a carrier. The guanidine eluates were injected onto a Vydac 300-Å $C_4$ reversed-phase column equilibrated with 0.1% trifluoroacetic acid and eluted using an acetonitrile gradient as described previously (*26*). Fractions were collected in 1-min intervals, and aliquots of each fraction were quantitated by scintillation counting. Unused portions were stored at −20 °C for further characterization.

*SDS−PAGE and Autoradiography.* Radiolabeled GPH-α forms that adsorbed to protein A−Sepharose beads were prepared as described previously (*25*). Briefly, GPH-α was eluted with twice-concentrated SDS gel sample buffer (125 mM Tris-HCl, pH 6.8, containing 2% SDS, 2% $\beta$-mercaptoethanol, 20% glycerol, and 40 $\mu$g/mL bromophenol blue). Samples were boiled for 5 min, loaded on polyacrylamide gradient slab gels (5−20%), and run by the method of Laemmli (*27*). The gels were dried in vacuo on filter paper and exposed to a phosphor screen (Molecular Dynamics). The phosphor screen was scanned on a Molecular Dynamics Storm 860, and bands were quantitated using the Molecular Dynamics ImageQuaNT (version 5.0) volume report.

*Amino Acid Analysis To Determine S−S Bond Content.* A modified protocol, similar to that used in determining the S−S folding pathways for potato carboxypeptidase inhibitor (*28*) and human epidermal growth factor (*29*), was used. [$^{35}$S]-Cysteine/cystine-containing folding forms isolated from reversed-phase HPLC were dried in vacuo and hydrolyzed as described previously (*6*). Quantitation of [$^{35}$S]cystine and succinyl[$^{35}$S]cysteine (hydrolysis product of NEM-alkylated cysteine residues) was performed using a modification of the method described by Cohen and Michaud (*30*). Hydrolysates were resuspended in 10 $\mu$L of 10 mM HCl. To this was added 70 $\mu$L of 0.2 N borate buffer, pH 8.8. Derivatization of amino acids was performed by adding 30 $\mu$L of 6-aminoquinolyl-*N*-hydroxysuccinimidyl carbamate (8 mg/mL in anhydrous acetonitrile). Samples were dried in vacuo. Before injection, samples were resuspended in 110 $\mu$L of buffer A (140 mM sodium acetate, 17 mM triethylamine, pH 4.9). Derivatized amino acids were separated by gradient elution as described previously (*6*) using buffer A and buffer B (60% acetonitrile in water). The column was eluted at 1.0 mL/min at 30 °C, and 1-mL fractions were collected and quantitated by scintillation counting. The peak containing [$^{35}$S]cystine represented cysteine residues involved in a S−S bond, whereas the peak containing succinyl[$^{35}$S]cysteine represented unformed S−S bonds. The percentage of [$^{35}$S]-cystine and succinyl[$^{35}$S]cysteine was calculated by dividing the cpm recovered for each species by the total cpm recovered. Fully folded [$^{35}$S]cysteine-labeled hCG-$\beta$ was used as a positive control for [$^{35}$S]cystine content.

## RESULTS

*Characterization of GPH-α Containing Only the Cystine Knot S−S Bonds.* Previously (*6*), we reported that removal of S−S bonds 7−31 and 59−87 does not affect the folding or secretion of GPH-α and demonstrated that the three cystine knot bonds (Figure 1) are necessary and sufficient for folding. The GPH-α variant containing only the cystine knot S−S bonds was termed $\alpha_k$. In the experiments described below, we used $\alpha_k$ and related mutants to determine the mechanism of cystine knot formation.

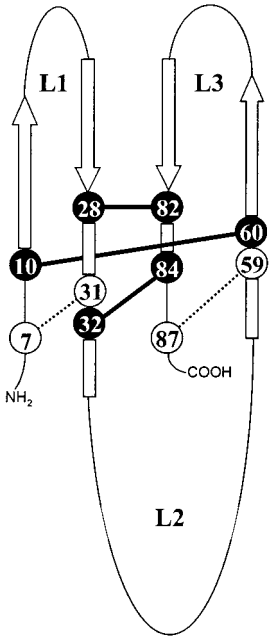


FIGURE 1: Schematic diagram of GPH-α. The crystal structure (*1*, *2*) of GPH-α indicates that the native conformation contains five S−S bonds: 7−31, 10−60, 28−82, 32−84, and 59−87. These S−S bonds stabilize the three-loop topology of GPH-α. The three loops are L1, L2, and L3. The cysteine residues displayed as filled circles form a cystine knot motif; 28−82 and 32−84 form a ring structure through which 10−60 penetrates. 7−31 and 59−87 (open circles and dotted lines) are non-cystine knot S−S bonds present in the N-terminal loop 1 domain and the C-terminal loop 3 domain, respectively.

Exposure of 293T cells to 2 mM DTT reversibly inhibits GPH-α S−S bond formation (*6*). Importantly, DTT treatment appears to have no effect on glycosylation, vesicular transport, or secretion of non-S−S containing proteins (*31*). To block the onset of S−S bond formation in pulse−chase experiments, 2 mM DTT was used during the pulse period (*6*, *31*). This strategy allowed for characterization of folding intermediates during the chase because removal of DTT permits S−S bond formation to proceed. The folding intermediates of $\alpha_k$ isolated by reversed-phase HPLC following a 10-min pulse in the presence of DTT and chases of 0−5 min in the absence of DTT are shown in Figure 2A. As previously reported, the 0-min chase resulted in the isolation of one peak (U) that represents unfolded $\alpha_k$ and contains no S−S bonds (*6*). Chase times of 30 s and 1 min show progression through an intermediate ($I_1$) to the fully folded conformation (F). Thus, the formation of the cystine knot proceeded through only one detectable intermediate, $I_1$. As with WT GPH-α (*6*), a 5-min chase resulted in complete U→F conversion.

To further characterize $I_1$ and F shown in Figure 2A, HPLC fractions containing each respective species were isolated and analyzed for the percentage of [$^{35}$S]cystine (i.e., S−S-linked cysteine residues) and succinyl[$^{35}$S]cysteine (i.e., the hydrolysis product of NEM-[$^{35}$S]cysteine, representing non-S−S-linked cysteine residues; see Experimental Proce-

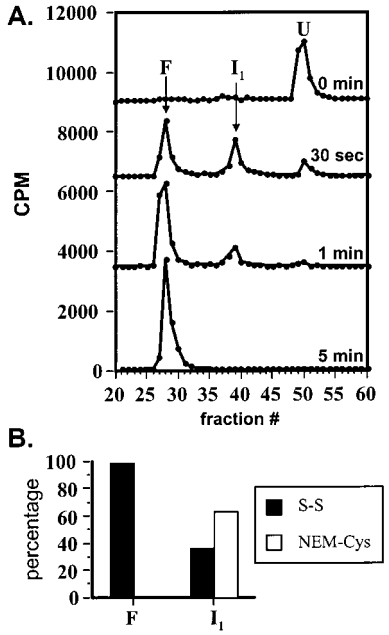


FIGURE 2: Analysis of $\alpha_k$ folding. 293T cells transiently transfected with pcDNA3-$\alpha_k$ were pulse-labeled with [$^{35}$S]cysteine for 10 min in the presence of 2 mM DTT followed by the chase times indicated after DTT removal. (A) HPLC profiles of $\alpha_k$ after no chase (0 min), 30 s, 1 min, and 5 min (baseline CPM have been offset for clarity). The elution position of unfolded $\alpha_k$ (U) was at about 50 min. The intermediate ($I_1$) and fully folded (F) species were isolated from HPLC, and the percentage of [$^{35}$S]cystine (S−S) and NEM-alkylated [$^{35}$S]cysteine (NEM-Cys) was determined as described under Experimental Procedures and is shown in (B). Recovery of 99.3% of $^{35}$S as cystine for F confirmed that all three S−S bonds were formed. Recovery of 36.3% of $^{35}$S as cystine for $I_1$ indicated that this intermediate contained one S−S bond and two unformed S−S bonds. The S−S content shown in each bar graph is the average of three independent experiments with standard deviations listed in Table 1.

dures). This assay quantitates the percentage of S−S bonds formed in each species. Shown in Figure 2B and Table 1 are the percentages of S−S bonded and nonbonded (NEM-alkylated) cysteine residues. $\alpha_k$ -F contained 99% of the $^{35}$S-radiolabel as cystine, indicating that all three possible bonds were intact. $\alpha_k$ $I_1$ contained 36% cystine, demonstrating that $I_1$ was a one-disulfide intermediate. Therefore, formation of the GPH-α cystine knot proceeds through a single observable one-disulfide intermediate that rapidly progresses to a fully folded form containing all three cystine knot S−S bonds.

*Order of Cystine Knot S−S Bond Formation.* Since cystine knot formation proceeded through a stable one-disulfide intermediate, $I_1$, identification of the one S−S bond would indicate the first bond to form in the GPH-α cystine knot. To identify this bond, a number of experiments were performed. First, site-directed mutagenesis was used to convert each $\alpha_k$ S−S pair to alanine. The three mutants created were $\alpha_k$C28−82A, $\alpha_k$C10−60A, and $\alpha_k$C32−84A. 293T cells transiently expressing each of these three mutants were pulse-labeled with [$^{35}$S]cysteine for 10 min in the presence of DTT and chased for 5 min in the absence of DTT. $\alpha_k$C28−82A remained in a conformation that eluted at the position of U (Figure 3A). The S−S content of $\alpha_k$-C28−82A(U) was <1% (Table 1), demonstrating that no S−S bonds had formed. Further conversion of U to a S−S bond-containing species was not observed at chase times of up to 30 min (data not shown). These data suggest that 28−82 is the first S−S bond to form within the cystine knot. S−S bond 10−60 would likely form second because it penetrates the cystine knot ring, making its formation sterically unfavorable after ring closure. Accordingly, 32−84 would then be the final S−S bond to form, completing the cystine knot.

Table 1: Quantitation of S−S Content in GPH-α Folding Intermediates[a]

| GPH-α variant | S−S[b] (%) | NEM-Cys[b] (%) | no. of S−S bonds[c] |
|---|---|---|---|
| $\alpha_k$ | | | |
| $I_1$ | 36.3 ± 8.1 | 63.7 ± 8.1 | 1.1 (3) |
| F | 99.3 ± 0.5[d] | 0.7 ± 0.5[d] | 3.0 (3)[d] |
| $\alpha_k$C28−82A | | | |
| U | 0.5 ± 0.7 | 99.5 ± 0.7 | 0.0 (2) |
| $\alpha_k$C32−84A | | | |
| $I_2$ | 97.7 ± 3.2 | 2.3 ± 3.2 | 2.0 (2) |
| $\alpha_k$C10−60A/C32−84A | | | |
| U′ | 1.9 ± 1.3 | 98.1 ± 1.3 | 0.0 (1) |
| $I_1$′ | 94.3 ± 2.4 | 5.7 ± 2.4 | 0.9 (1) |
| α7−31/59−87 | | | |
| U | 7.8 ± 2.4 | 92.2 ± 2.4 | 0.2 (2) |
| $I_A$ | 43.6 ± 3.0 | 56.4 ± 3.0 | 0.9 (2) |
| α(GlyL2) | | | |
| F | 98.0 ± 1.8 | 2.0 ± 1.8 | 4.9 (5) |
| α-WT | | | |
| N | 98.7 ± 0.9[d] | 1.2 ± 0.7[d] | 4.9 (5)[d] |

[a] Amino acid analysis was used to determine the relative amount of S−S bond formation. The folding species correspond to the intermediates referred to on the HPLC chromatograms in Figures 2−4 and 6. Shown are the calculated percentages of S−S bond formation (S−S), unformed S−S bonds (NEM-Cys), and the calculated number of S−S bonds formed. [b] Average of at least 3 independent experiments ± SD. [c] Calculated as percentage S−S × total possible disulfide bonds that could theoretically form. The number in parentheses denotes the total possible S−S bonds for each GPH-α variant. [d] Data from previous report (*6*).

If the order of S−S bond formation within the GPH-α knot is indeed 28−82→10−60→32−84, then three conditions should be met. First, a mutant containing only Cys28 and Cys82 should generate a folding form that elutes from HPLC at the same position as $I_1$. Second, removal of S−S bond 32−84 ($\alpha_k$C32−84A) should result in the formation of a two-disulfide species (containing the first two bonds; 28−82 and 10−60) that elutes from HPLC at a position between $I_1$ and F (see Figure 2A). Normally, this two-disulfide intermediate must be short-lived, since it was not detected during $\alpha_k$ folding (Figure 2A). Third, progression to the $\alpha_k$C32−84A two-disulfide intermediate should progress through the one-disulfide intermediate $I_1$.

To test the first prediction, a mutant containing only Cys28 and Cys82 (termed $\alpha_k$C10−60A/C32−84A) was constructed, expressed in 293T cells, and pulse-labeled for 10 min followed by a 10-min chase. Shown in Figure 3B (solid line) is the conversion from an unfolded species (U′) to a partially folded species (I′$_1$). I′$_1$ contained 94.3% of the $^{35}$S-radiolabel as cystine (Table 1), indicating that S−S bond 28−82 had formed in this species. The two folding species in Figure 3B were labeled U′ and I′ because they eluted 3 min earlier than $\alpha_k$ U and I, respectively (Figure 2A). Because the unfolded form, U′, was shifted 3 min relative to $\alpha_k$ U, we conclude that this shift resulted from a change in hydrophobicity caused by the four Cys→Ala substitutions. These four substitutions could alter the hydrophobicity of $\alpha_k$C10−60A/C32−84A intermediates because there are four fewer NEM-

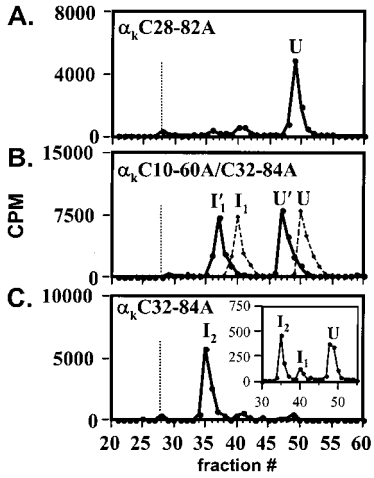


FIGURE 3: HPLC analysis of $\alpha_k$ S−S mutants. 293T cells transiently transfected with pcDNA3-$\alpha_k$ mutants were pulse-labeled with [$^{35}$S]-cysteine as indicated below. (A) HPLC profile of $\alpha_k$C28−82A pulse-labeled for 10 min in the presence of DTT and chased for 5 min after DTT removal. Chase times of greater than 5 min did not result in the formation of any additional peaks (data not shown). U represents the unfolded $\alpha_k$C28−82A containing no S−S bonds (Table 1). (B, solid line) HPLC profile of $\alpha_k$C10−60A/C32−84A (this mutant contains only Cys28 and Cys82) pulse-labeled for 10 min and chased for 10 min. The elution positions of the unfolded species (U′) and the intermediate ($I_1$′) were 3 min earlier than observed for $\alpha_k$ (Figure 2A) (see text). Correction for this difference is displayed as a dashed line. (C) HPLC profile of $\alpha_k$C32−84A pulse-labeled for 10 min in the presence of DTT and chased for 5 min after DTT removal. $\alpha_k$C32−84A folded to an intermediate ($I_2$) that contained both S−S bonds (Table 1). (C, inset) HPLC profile of $\alpha_k$C32−84A pulse-labeled for 10 min in the presence of DTT and chased for 30 s after DTT removal, demonstrating progression through the $I_1$ intermediate. Vertical dotted line, elution position of fully folded WT and $\alpha_k$.

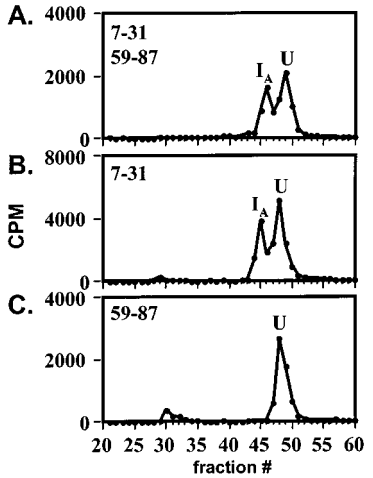


FIGURE 4: HPLC analysis of 7−31 and 59−87 formation in the absence of the cystine knot. Transiently transfected 293T cells were pulse-labeled with [$^{35}$S]cysteine for 10 min followed by a 10-min chase. HPLC was used to analyze the immunoprecipitated folding forms. The numbers in the upper left of each panel represent the cysteine residues present and the potential native bonds that could form. $I_A$ contained one S−S bond, and U contained no S−S bonds (Table 1).

alkylated cysteine residues than are present in $\alpha_k$ U and $I_1$ (Figure 2A). Adjustment of the HPLC trace for this difference (Figure 3B, dashed line) shows that the elution position of $\alpha_k$C10−60A/C32−84A $I_1$ is the same as that observed for $\alpha_k$ $I_1$ (Figure 2A). Chase times of >10 min resulted in about 70% U′→$I'_1$ conversion. These data support our first prediction that a GPH-α subunit containing only Cys28 and Cys82 forms a one-disulfide intermediate that elutes at the position of $\alpha_k$ $I_1$.

The second prediction was confirmed by construction of $\alpha_k$C32−84A, expression in 293T cells, and pulse-labeling for 10 min followed by a 5-min chase. $\alpha_k$C32−84A folded to a species (termed $I_2$) that eluted between $I_1$ and F (Figure 3C). Additionally, $I_2$ contained 97.7% of the $^{35}$S-radiolabel in the cystine form (Table 1), indicating that the two remaining S−S bonds (28−82 and 10−60) had formed. The final prediction was that formation of $\alpha_k$C32−84A $I_2$ should progress through the $I_1$ intermediate. To test this, 293T cells expressing $\alpha_k$C32−84A were labeled for 10 min in the presence of DTT and chased for 30 s in the absence of DTT. HPLC separation of the isolated folding forms (Figure 3C, inset) shows that folding to $I_2$ did progress through a short-lived intermediate that migrated at the same position as $I_1$ (Figure 2A). This provides further evidence that 32−84 is the last bond to form within the cystine knot.

Removal of S−S bond 10−60 (termed $\alpha_k$C10−60A), the second bond to form, resulted in an ensemble of at least four folding species that eluted from HPLC between 33 and 50 min (data not shown). Furthermore, about 20−25% of $\alpha_k$-C10−60A formed S−S-linked multimers that eluted at high acetonitrile concentrations. Reducing and nonreducing SDS−PAGE indicated that these forms were S−S-linked multimers since high molecular weight forms observed under nonreducing conditions collapsed to migrate at the locus of monomeric GPH-α under reducing conditions (data not shown). This aberrant folding of $\alpha_k$C10−60A may have occurred because the free thiols at Cys32 and Cys84 were unable to form a S−S bond in the absence of S−S bond 10−60. These free thiols may have formed interprotein S−S linkages such as those reported for hCG-*β* mutants containing free thiols that cannot form native S−S bonds (*14*).

*Role of the Cystine Knot in the Formation of S−S Bonds 7−31 and 59−87.* S−S bonds 7−31 and 59−87 are not part of the GPH-α cystine knot, but are present in the N- and C-terminal domains, respectively (Figure 1). NMR studies of unassembled GPH-α show that the N- and C-terminal domains containing loops 1 and 3 are structurally defined, whereas the structure of loop 2 is undefined (*15*, *16*). Thus, the flexible loop 2 appears to tether the N- and C-terminal domains, which may fold independently. Using S−S bond 7−31 and 59−87 formation as general indicators of folding for the respective N- and C-terminal domains, we asked the following question: Can S−S bonds 7−31 and 59−87 form in the absence of the cystine knot?

To answer this question, a GPH-α mutant containing only Cys7, Cys31, Cys59, and Cys 87 (termed α7−31/59−87) was constructed and characterized. Folding of α7−31/59−87 resulted in about 45% of the total protein rapidly converting from U to a folding intermediate termed $I_A$ (Figure 4A). About half of the $^{35}$S-radiolabel in $I_A$ was cystine, and the other half was derived from NEM-Cys (Table 1), indicating that one out of the two potential S−S bonds had formed. To identify this S−S bond, two additional mutants were constructed that each contained only two cysteine residues: those required for S−S bond 7−31 (termed α7−31) and those required for bond 59−87 (termed α59−87).

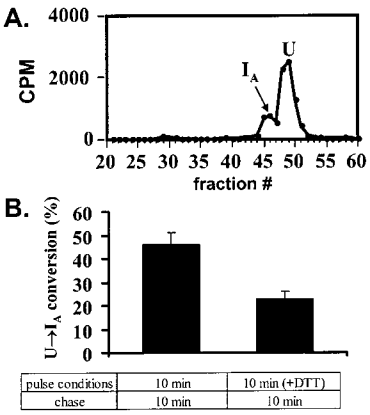


FIGURE 5: Efficiency of 7−31 formation with and without DTT treatment. 293T cells transiently transfected with pcDNA3-α7−31/59−87 were pulse-labeled as indicated below. (A) HPLC profile of α7−31/59−87 pulse-labeled for 10 min in the presence of DTT and chased for 10 min after DTT removal. These pulse/chase conditions differ from Figure 4A in that DTT was included in the pulse. U→$I_A$ conversion was complete within 1 min, and no further conversion occurred with longer chase times. (B) Quantitation of the percent U→$I_A$ conversion with or without DTT during the pulse. U→$I_A$ conversion is a measure of 7−31 formation (Figure 4). The bars represent the average of three independent experiments ± SD.

The HPLC profiles for these two mutants are shown in Figure 4B and Figure 4C, respectively. Folding of α7−31 was indistinguishable from α7−31/59−87, and α59−87 remained in its unfolded conformation. This indicates that S−S bond 7−31 was the bond that had formed in α7−31/59−87. From these data, we conclude that 7−31 can form independent of the cystine knot. Furthermore, formation of 59−87 is dependent upon the cystine knot.

When DTT is included in the pulse, formation of S−S bonds, but not translocation of nascent chains into the endoplasmic reticulum, is delayed until DTT removal (*6*, *31*). Thus, a consequence of DTT treatment is that the polypeptide accumulates in a reduced and unfolded form. Upon DTT removal, S−S bond formation and folding can proceed posttranslationally (*6*, *31*). Shown in Figure 5A is a HPLC profile of α7−31/59−87 following a 10-min pulse in the presence of DTT and a 10-min chase in the absence of DTT. The U→$I_A$ conversion was less efficient than that observed when DTT was not included during the pulse (compare Figures 4A and 5A). The inclusion of DTT during the pulse decreased U→$I_A$ conversion by about 2-fold (Figure 5B). Since U→$I_A$ conversion represents the formation of S−S bond 7−31, as shown in Figure 4, we conclude that 7−31 forms more efficiently when folding can occur during or immediately after polypeptide synthesis. Therefore, the data imply that S−S bond 7−31 is an early bond to form.

*Role of Loop 2 in GPH-α Folding, Secretion, and Assembly with hCG-β.* As alluded to above, the structure of GPH-α loop 2 is undefined in the unassembled subunit (*15*, *16*), and its role in folding is unknown. Based on its flexibility, we hypothesized that loop 2 plays a passive role in folding, primarily serving to tether the structurally defined N- and C-terminal domains. To test this hypothesis, we created an artificially flexible loop 2 by replacing residues 36−55 with 20 consecutive glycine residues [termed α-(GlyL2)]. Figure 6 lists the WT and α(GlyL2) loop 2 sequences. Note that the glycosylation site at Asn52 was also removed.

Following a 10-min pulse in the presence of DTT and a 2-min chase in the absence of DTT, the reversed-phase HPLC profile for WT GPH-α showed two peaks: a sharp peak at 28 min and a broad, heterogeneous peak that eluted from 31 to 45 min (Figure 6A). The broad peak rapidly converted to the 28-min peak and represents native GPH-α, which contains five S−S bonds (Table 1). The similarity between the rate, the extent of folding, and the HPLC profiles for WT and α(GlyL2) is striking (Figure 6, compare panel A with panel B). Additionally, the fully folded form of α-(GlyL2) (Figure 6B, 5 min) and the native WT-α each contained five S−S bonds (Table 1). The only detectable difference was that the fully folded form of α(GlyL2) eluted 2 min later than native WT-α (30 min versus 28 min, respectively). However, unfolded α(GlyL2) also eluted 2 min later than unfolded WT (52 min versus 50 min; data not shown). Because the elution times of both the unfolded and the folded forms were shifted by 2 min, the change is most likely due to a hydrophobicity change caused by replacement of the WT loop 2 with glycine. Further support for this interpretation was obtained when we calculated the relative hydrophobicity of the 20 glycine residues in α(GlyL2) and the WT residues 36−55 using the Kyte and Doolittle method (*32*). The value obtained for WT was −11.7, compared to −8.0 for α(GlyL2). The higher calculated value for α(GlyL2) indicates that the glycine sequence is expected to be more hydrophobic relative to the corresponding WT residues. Because the affinity of protein binding to a reversed-phase HPLC column is a function of its hydrophobicity, α(GlyL2) would be expected to elute later than WT, as observed in Figure 6A,B.

Translocation through the quality control system of the endoplasmic reticulum and efficient secretion are other indicators of proper folding [reviewed in (*33*, *34*)]. To determine the efficiency of secretion, 293T cells expressing WT or α(GlyL2) were pulse-labeled for 10 min and chased for 10 min or 8 h. SDS−PAGE analysis and quantitation of band density demonstrated that secretion of WT and α-(GlyL2) were comparable (70−80%) (Figure 6C). The lower molecular weight of α(GlyL2) was due to the absence of the Asn52-oligosaccharide. These data provide additional evidence that α(GlyL2) folds properly. Additionally, these data demonstrate that the Asn52-oligosaccharide is not necessary for GPH-α folding or secretion. GPH-α loop 2 interacts with hCG-β upon dimer formation; residues 36−41 (*8*, *35*) and the oligosaccharide at Asn52 (*36*) are particularly important, and since these residues were converted to glycine, α(GlyL2) did not assemble with hCG-β (data not shown).

## DISCUSSION

The GPH-α cystine knot motif, the two non-cystine knot S−S bonds, and the loop 2 domain were studied to establish the mechanism of GPH-α folding. The cystine knot motif was studied using a mutant ($\alpha_k$) that contained only the six cysteine residues that form the cystine knot S−S bonds. Based on our intracellular folding data, the hCG crystal structure (*1*, *2*), and the NMR structure of unassembled GPH-α (*15*, *16*), we present the following model for GPH-α folding. This extends our laboratories previous reports for hCG-β folding (*7*, *25*, *26*, *37*, *38*) to include its dimeric partner, GPH-α. Understanding the folding of GPH-α and

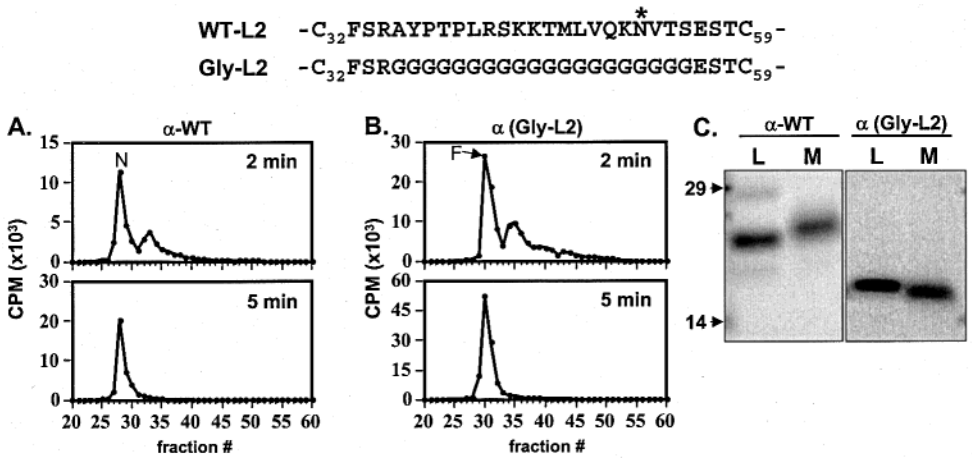


FIGURE 6: Comparison of WT GPH-α and α(GlyL2). WT loop 2 and residues replaced by glycine in α(GlyL2) are listed at the top. The asterisk at Asn52 in WT represents the position of an N-linked oligosaccharide. (A and B) Respective HPLC profiles of WT GPH-α and α(GlyL2) pulse-labeled for 10 min in the presence of DTT and chased for 2 or 5 min after DTT removal. The native conformation of WT-α (N) and fully folded α(GlyL2) (F) are indicated. α(GlyL2)-F was not designated as 'native' because the conformation attained by Gly loop 2 is unknown. (C) secretion of WT and α(GlyL2) analyzed by reducing SDS−PAGE and autoradiography. The lysate (L) represents the total intracellular [$^{35}$S]cysteine-labeled GPH-α after a 10-min pulse and 10-min chase. The amount of radioactivity in this band was used as the "initial cpm" when calculating the amount secreted into the medium (M) after 8 h. Less than 5% of the total GPH-α remained intracellular after 8 h (data not shown). The higher apparent molecular weight of secreted WT (compared to intracellular) was a result of differential processing of the two N-linked oligosaccharides (*44*) and addition of O-linked oligosaccharides (*45*) to the unassembled GPH-α. The faster migration of α(GlyL2) was due to the absence of the N-linked oligosaccharide at Asn52. Molecular weight marker 29 is carbonic anhydrase ($M_r$ = 29 000) and 14 is lysozyme ($M_r$ = 14 300).

hCG-*β*, both of which are members of a superfamily of cystine knot proteins, should aid in future investigations into structure/function relationships of other cystine knot-containing proteins.

Pulse−chase studies employing $\alpha_k$ demonstrated that formation of the GPH-α cystine knot proceeded through a one-disulfide intermediate. Data from a series of mutants suggest that the bond formed in the one-disulfide intermediate is 28−82, and thus imply that 28−82 is the first S−S bond to form within the cystine knot. Lack of an observable two-disulfide intermediate suggests that formation of the second S−S bond is rapidly followed by formation of the third bond. Disulfide bonds 10−60 and 32−84 appeared to form second and third, respectively. Thus, formation of the penetrating bond in the cystine knot (10−60) appears to be the rate-limiting step. Based on earlier observations, this order of cystine knot S−S formation (i.e., 28−82→10−60→32−84) might have been anticipated. As described above, loop 2 has an undefined conformation in the unassembled subunit (*15, 16*). Thus, GPH-α folding is likely to be driven by the formation of its structurally defined regions (i.e., loops 1 and 3). Interactions between loops 1 and 3 (see Figure 1) could stabilize a conformation that allows the S−S bond closest to this interaction (bond 28−82) to form. The identification of 28−82 as the first bond to form within the cystine knot supports this idea; 28−82 is near interaction sites between loops 1 and 3 and bridges these two domains. As folding progresses, formation of 10−60 and 32−84 follow.

S−S bonds 7−31 and 59−87, although not required for subunit folding or secretion (*6*), are important for the multiple roles of GPH-α in the biological function of the glycoprotein hormones (*39, 40*). To determine if formation of these two bonds can occur independent of the cystine knot, we monitored their ability to form when all three cystine knot bonds were absent. Our hypothesis was that both bonds would form independent of the knot. This was based on the observation that the N-terminal loop 1 domain (containing 7−31) and the C-terminal loop 3 domain (containing 59−87) are connected by the flexible loop 2. Thus, these domains might fold independently. However, S−S bond 7−31, but not 59−87, formed in the absence of the cystine knot. The formation of 7−31 indicates that loop 1 had formed a native or nativelike conformation independent of the cystine knot. The inability of S−S bond 59−87 to form in the absence of the cystine knot may indicate that the C-terminal loop 3 domain cannot form a nativelike conformation until it is stabilized by some or all of the cystine knot. Therefore, we conclude that 59−87 formation occurs during or after cystine knot formation.

Another potential folding domain investigated was loop 2. The hypothesis that we tested was that the flexible loop 2 does not play an active role in folding, but rather is a byproduct of the folding and interaction of loops 1 and 3. Replacing nearly all of loop 2 (residues 36−55) with an artificially flexible glycine chain had little effect on the profile of intermediates, on the kinetics of folding, or on subunit secretion. This suggests that GPH-α folding is not dependent upon the native sequence of loop 2 and is consistent with our hypothesis that loop 2 does not actively participate in folding. With many potential interactions involving loop 2, the fact that no effect was seen when loop 2 was replaced with a glycine chain further demonstrates the passive nature of this loop during folding of the free subunit. These results also suggest that GPH-α folding fits a diffusion−collision model (*17*) in which the flexible loop 2 connects the structurally defined N- and C-terminal domains. In this model, the two terminal domains would diffuse randomly until the proper collision is stabilized by interdomain interactions, such as S−S bond formation. The position of S−S bond 28−82 (connecting the N- and C-terminal GPH-α domains) and the fact that it is the first bond to form within the cystine knot are consistent with this model. Thus, loop 2 appears to be formed when the loop 1

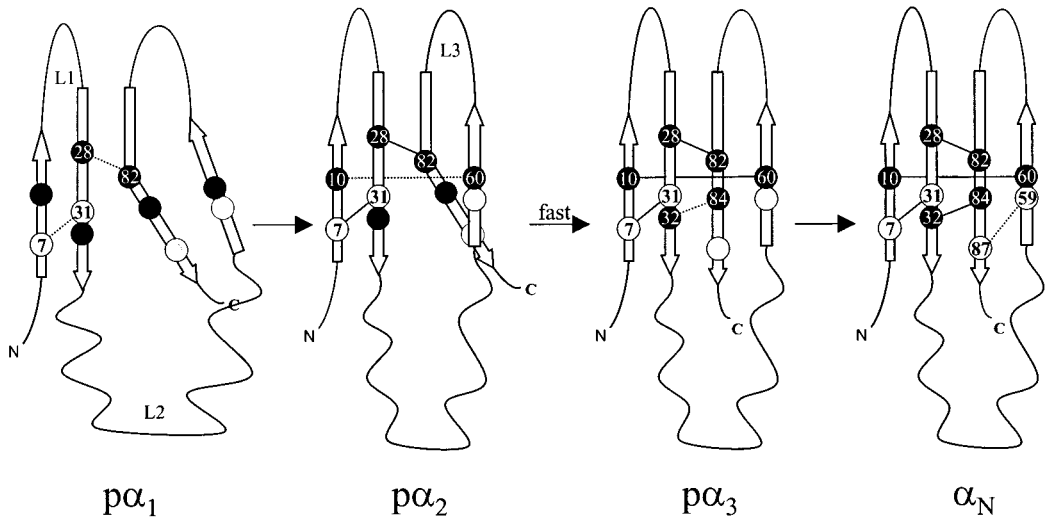


FIGURE 7: GPH-α intracellular folding pathway. Details and rationale for the above model are described under the *GPH-α Intracellular Folding Pathway* section of the Discussion. The four open circles and six filled circles represent cysteine residues that form two non-cystine knot and three cystine knot S−S bonds, respectively. Dotted lines connecting cysteine residues depict newly formed S−S bonds in each intermediate, and solid lines represent previously formed S−S bonds. pα designates precursor forms of GPH-α that progress toward the native conformation ($\alpha_N$), which contains all five S−S bonds. L1, L2, and L3 represent the three GPH-α loops. The squiggly line for L2 resembles its undefined conformation in the unassembled subunit (*15, 16*).

and loop 3 domains interact and are stabilized by formation of the cystine knot. In this capacity, loop 2 plays a passive role in GPH-α folding rather than being an active driving force.

The amino acid sequence and flexible nature of loop 2 appear to permit assembly of GPH-α with four glycoprotein hormone *β*-subunits. Furthermore, loop 2 residues required for biological activity vary between the glycoprotein hormones. For example, Phe33, Arg35, and Lys44 of GPH-α loop 2 are critical for high-affinity hCG receptor binding, but none of these residues are important for follicle-stimulating hormone receptor binding (*35, 41*). Additionally, the removal of the N-linked oligosaccharide at Asn52 disrupts hCG bioactivity (*42*), but has no effect on thyroid-stimulating hormone bioactivity (*43*). These data, along with ours, support the evolving idea that GPH-α loop 2 has multiple functions that are determined by the interaction with four hormone-specific *β*-subunits. Thus, the biological specificity of the glycoprotein hormones may be, at least in part, due to *β*-subunit stabilization of different GPH-α loop 2 conformations. More detailed structural studies comparing the final conformation of loop 2 in the four hormones are needed to further test this hypothesis.

*GPH-α Intracellular Folding Pathway.* Figure 7 depicts a model for GPH-α folding. The conformations of the folding intermediates are drawn to emphasize the regions of GPH-α that may form during folding, but do not suggest actual structures. At designated steps along the folding pathway, we have shown how the convergence of various domains may occur as S−S bonds form to stabilize intermediates, allowing subsequent S−S bonds to form. The folding pathway described in Figure 7 depicts what we believe are the most likely progression of the most populated folding intermediates.

S−S bond 7−31 formed more efficiently in the absence of the cystine knot when S−S bond formation was not initially inhibited with DTT, suggesting that 7−31 forms during or rapidly after protein synthesis. However, only about half of 7−31 formed in the absence of the cystine knot, demonstrating that the efficiency of 7−31 decreases when the cystine knot is removed. There are at least two possible explanations for this result. First, if 7−31 is not allowed to form rapidly after protein synthesis, GPH-α may have a greater propensity to become a trapped intermediate. Second, the two species (U and $I_A$) may reach an equilibrium state. Shifting of this equilibrium toward the native conformation may only occur if subsequent S−S bonds can form. The first bond to form within the cystine knot was 28−82. Although S−S bond 7−31 appears to have the potential to form first, therefore preceding 28−82 formation, these two S−S bonds can form independently. Therefore, we have included both of these bonds in the earliest folding intermediate (termed $p\alpha_1$, where p indicates a precursor to the mature GPH-α) (Figure 7).

The intermediate containing 28−82 (Figure 2A, $I_1$) rapidly converted to a form containing all three cystine knot bonds. In Figure 7, $p\alpha_2$ shows the formation of 10−60, followed by rapid closure of knot with 32−84 formation ($p\alpha_3$). Based on our data, the formation of S−S bond 59−87 is dependent upon some or all of the cystine knot being present. Thus, 59−87 forms either during or after cystine knot formation. One possibility is after S−S bond 10−60 forms because Cys59 is next to Cys60 and could be drawn into the proximity of Cys87. However, we believe that 59−87 forms after completion of the knot because: (i) the third S−S bond of the cystine knot (32−84) forms very rapidly after 10−60 (as discussed above); (ii) formation of 32−84 may stabilize the otherwise flexible C-terminus (*15*), allowing for 59−87 formation; and (iii) removal of 59−87 alone does not affect the formation of the other four S−S bonds, whereas removal of 32−84 does (*6*).

Although GPH-α and hCG-*β* have no apparent amino acid sequence similarity, they do share a common three-loop antiparallel topology that is stabilized by a cystine knot (*1*). This structural topology is also observed in a number of other growth factors (*4, 5*). Our understanding of hCG-*β* and GPH-α folding has revealed some commonalties in the folding of these two cystine knot proteins. Examples

include: (i) the first S−S bonds to form within the cystine knots are equivalent, (ii) formation of the loop 1 domain appears to be an early event in folding, followed by the formation of the cystine knot, and (iii) formation of loop 2 appears to be a byproduct of folding. Based on the commonalties in the folding pathways for GPH-α and hCG-*β*, as well as the similarities in the topology and dimeric nature shared with other cystine knot proteins, we propose that many of these proteins fold by similar mechanisms and pathways. More detailed studies aimed at understanding the folding of cystine knot proteins outside of the glycoprotein hormone family may further test this hypothesis.

## ACKNOWLEDGMENT

We gratefully acknowledge Drs. Angie Rizzino, Larry Schopfer, and Oksana Lockridge for experimental suggestions and Dr. Simon Sherman for reviewing the manuscript. We also acknowledge the Eppley Institute Molecular Biology Core Lab for primer synthesis and DNA sequencing and Dr. Fulvio Perini for technical assistance in performing amino acid analysis.

## REFERENCES

1. Lapthorn, A. J., Harris, D. C., Littlejohn, A., Lustbader, J. W., Canfield, R. E., Machin, K. J., Morgan, F. J., and Isaacs, N. W. (1994) *Nature 369*, 455.
2. Wu, H., Lustbader, J. W., Liu, Y., Canfield, R. E., and Hendrickson, W. A. (1994) *Structure 2*, 545.
3. Sun, P. D., and Davies, D. R. (1995) *Annu. Rev. Biophys. Biomol. Struct. 24*, 269.
4. Isaacs, N. W. (1995) *Curr. Opin. Struct. Biol. 5*, 391.
5. Muller, Y. A., Christinger, H. W., Keyt, B. A., and de Vos, A. M. (1997) *Structure 5*, 1325.
6. Darling, R. J., Ruddon, R. W., Perini, F., and Bedows, E. (2000) *J. Biol. Chem. 275*, 15413.
7. Bedows, E., Huth, J. R., Suganuma, N., Bartels, C. F., Boime, I., and Ruddon, R. W. (1993) *J. Biol. Chem. 268*, 11655.
8. Bielinska, M., and Boime, I. (1992) *Mol. Endocrinol. 6*, 261.
9. Sato, A., Perlas, E., Ben-Menahem, D., Kudo, M., Pixley, M. R., Furuhashi, M., Hsueh, A. J., and Boime, I. (1997) *J. Biol. Chem. 272*, 18098.
10. Strasberg, P., Liede, H. A., Stein, T., Warren, I., Sutherland, J., and Ray, P. N. (1995) *Hum. Mol. Genet. 4*, 2179.
11. Schuback, D. E., Chen, Z. Y., Craig, I. W., Breakefield, X. O., and Sims, K. B. (1995) *Hum. Mutat. 5*, 285.
12. Hayashizaki, Y., Hiraoka, Y., Endo, Y., Miyai, K., and Matsubara, K. (1989) *EMBO J. 8*, 2291.
13. Daly, N. L., and Craik, D. J. (2000) *J. Biol. Chem. 275*, 19068.
14. Bedows, E., Norton, S. E., Huth, J. R., Suganuma, N., Boime, I., and Ruddon, R. W. (1994) *J. Biol. Chem. 269*, 10574.
15. Erbel, P. J., Karimi-Nejad, Y., Beer, T. D., Boelens, R., Kamerling, J. P., and Vliegenthart, J. F. (1999) *Eur. J. Biochem. 260*, 490.
16. De Beer, T., Van Zuylen, C. W., Leeflang, B. R., Hard, K., Boelens, R., Kaptein, R., Kamerling, J. P., and Vliegenthart, J. F. (1996) *Eur. J. Biochem. 241*, 229.
17. Karplus, M., and Weaver, D. L. (1994) *Protein Sci. 3*, 650.
18. Nagi, A. D., and Regan, L. (1997) *Fold. Des. 2*, 67.
19. Nagi, A. D., Anderson, K. S., and Regan, L. (1999) *J. Mol. Biol. 286*, 257.
20. Ladurner, A. G., and Fersht, A. R. (1997) *J. Mol. Biol. 273*, 330.
21. Viguera, A. R., and Serrano, L. (1997) *Nat. Struct. Biol. 4*, 939.
22. Pear, W. S., Nolan, G. P., Scott, M. L., and Baltimore, D. (1993) *Proc. Natl. Acad. Sci. U.S.A. 90*, 8392.
23. Suganuma, N., Matzuk, M. M., and Boime, I. (1989) *J. Biol. Chem. 264*, 19302.
24. Sarkar, G., and Sommer, S. S. (1990) *BioTechniques 8*, 404.
25. Bedows, E., Huth, J. R., and Ruddon, R. W. (1992) *J. Biol. Chem. 267*, 8880.
26. Huth, J. R., Mountjoy, K., Perini, F., and Ruddon, R. W. (1992) *J. Biol. Chem. 267*, 8870.
27. Laemmli, U. K. (1970) *Nature 227*, 680.
28. Chang, J. Y., Canals, F., Schindler, P., Querol, E., and Aviles, F. X. (1994) *J. Biol. Chem. 269*, 22087.
29. Chang, J. Y., Schindler, P., Ramseier, U., and Lai, P. H. (1995) *J. Biol. Chem. 270*, 9207.
30. Cohen, S. A., and Michaud, D. P. (1993) *Anal. Biochem. 211*, 279.
31. Lodish, H. F., and Kong, N. (1993) *J. Biol. Chem. 268*, 20598.
32. Kyte, J., and Doolittle, R. F. (1982) *J. Mol. Biol. 157*, 105.
33. Ellgaard, L., Molinari, M., and Helenius, A. (1999) *Science 286*, 1882.
34. Ruddon, R. W., and Bedows, E. (1997) *J. Biol. Chem. 272*, 3125.
35. Xia, H., Chen, F., and Puett, D. (1994) *Endocrinology 134*, 1768.
36. Matzuk, M. M., and Boime, I. (1988) *J. Cell Biol. 106*, 1049.
37. Beebe, J. S., Mountjoy, K., Krzesicki, R. F., Perini, F., and Ruddon, R. W. (1990) *J. Biol. Chem. 265*, 312.
38. Huth, J. R., Perini, F., Lockridge, O., Bedows, E., and Ruddon, R. W. (1993) *J. Biol. Chem. 268*, 16472.
39. Furuhashi, M., Ando, H., Bielinska, M., Pixley, M. R., Shikone, T., Hsueh, A. J., and Boime, I. (1994) *J. Biol. Chem. 269*, 25543.
40. Furuhashi, M., Suzuki, S., and Suganuma, N. (1996) *Endocrinology 137*, 4196.
41. Liu, C., Roth, K. E., Shepard, B. A., Shaffer, J. B., and Dias, J. A. (1993) *J. Biol. Chem. 268*, 21613.
42. Matzuk, M. M., Keene, J. L., and Boime, I. (1989) *J. Biol. Chem. 264*, 2409.
43. Fares, F. A., Gruener, N., and Kraiem, Z. (1996) *Endocrinology 137*, 555.
44. Corless, C. L., Bielinska, M., Ramabhadran, T. V., Daniels-McQueen, S., Otani, T., Reitz, B. A., Tiemeier, D. C., and Boime, I. (1987) *J. Biol. Chem. 262*, 14197.
45. Peters, B. P., Krzesicki, R. F., Perini, F., and Ruddon, R. W. (1989) *Endocrinology 124*, 1602.

BI002046A